

ORIGINAL RESEARCH

# Molecular and Cellular Differences in Cardiac Repair of Male and Female Mice

Amanda B. Pullen, BS; Vasundhara Kain, PhD; Charles N. Serhan, PhD, DSc; Ganesh V. Halade , PhD

**BACKGROUND:** Leukocyte-directed biosynthesis of specialized proresolving mediators (SPMs) orchestrates physiological inflammation after myocardial infarction. Deficiency of SPMs drives pathological and nonresolving inflammation, leading to heart failure (HF). Differences in SPMs and inflammatory responses caused by sex-specific differences are of interest. We differentiated leukocyte-directed biosynthesis of lipid mediators in male and female mice, focusing on leukocyte populations, structural remodeling, functional recovery, and survival rates.

**METHODS AND RESULTS:** Risk-free male and female C57BL/6 mice were selected as naïve controls or subjected to myocardial infarction surgery. Molecular and cellular mechanisms that differentiate survival, heart function, and structure and leukocyte-directed lipid mediators were quantified to describe physiological inflammation after myocardial infarction. Female mice show improved survival in acute HF but no statistical difference during chronic HF compared with male mice. Female mice improved survival is marked with functional recovery and limited remodeling compared with male mice. Male and female mice are similarly responsive to arachidonate lipoxygenase (*LOX-5*, *LOX-12*, *LOX-15*) or cyclooxygenase (*COX-1*, *COX-2*) in acute HF and particularly male infarcted heart had overall increased SPMs. Female cardiac healing is marked with the biosynthesis of differential p450-derived product, particularly 11,12 epoxyeicosatrienoic acid in acute HF. A sex-specific difference of dendritic cells in acute HF is distinct, with limited changes in chronic HF.

**CONCLUSIONS:** Cardiac repair is marked with increased SPM biosynthesis in male mice and amplified epoxyeicosatrienoic acid in female mice. Female mice showed improved survival, functional recovery, and limited remodeling, which are signs of fine-tuned physiological inflammation after myocardial infarction. These results rationalize the sex-specific precise therapies and differential treatments in acute and chronic HF.

**Key Words:** heart failure ■ ischemia ■ leukocytes ■ resolution of inflammation ■ specialized proresolving mediators

**C**ardiovascular disease (CVD) is a leading cause of death in the United States, with close to one third of deaths being attributed to some form of cardiometabolic pathological feature.<sup>1,2</sup> The primary risk factors for CVD are related to several lifestyle aspects that increase the likelihood of myocardial infarction (MI; heart attack) in men and women. MI events are less common in premenopausal women and occur in men at an earlier age ( $\approx 65$  years) compared with women ( $\approx 72$  years).<sup>3-5</sup> The epidemiological study on the autonomic response to CVD compounded with obesity showed, although men and women are both

negatively impacted by obesity, some cellular and molecular mechanisms of these responses are sex specific and the overall mechanism is incomplete.<sup>6</sup> There are differences in the risk, timing, and symptoms of heart disease between men and women for a variety of pathological conditions; however, estrogen has been linked to a higher survival rate of cardiomyocytes after MI.<sup>7</sup> Sex-specific differences in cardiovascular health stem from multiple factors, including leukocytes, fat immune metabolism, glycoprotein content, gene expression, sex hormones, and sociocultural aspects, like behavior, environment, and nutrition.<sup>8-11</sup>

Correspondence to: Ganesh V. Halade, PhD, Division of Cardiovascular Sciences, Department of Medicine, University of South Florida, 560 Channelside Dr, Tampa, FL 33602. E-mail: ghalade@usf.edu

Supplementary Materials for this article is available at <https://www.ahajournals.org/doi/suppl/10.1161/JAHA.119.015672>

For Sources of Funding and Disclosures, see page 14.

© 2020 The Authors. Published on behalf of the American Heart Association, Inc., by Wiley. This is an open access article under the terms of the Creative Commons Attribution-NonCommercial License, which permits use, distribution and reproduction in any medium, provided the original work is properly cited and is not used for commercial purposes.

JAHA is available at: [www.ahajournals.org/journal/jaha](http://www.ahajournals.org/journal/jaha)

## CLINICAL PERSPECTIVE

### What Is New?

- Leukocyte influx coordinates the biosynthesis of specialized proresolving mediators for resolution of inflammation and timely cardiac repair after myocardial infarction.
- In response to massive infarcts in male and female mice, leukocytes express higher levels of lipoxygenase (5, 12, and 15) in the spleen and heart, orchestrating the comprehensive bioactive lipid remodeling that is essential for the resolution of inflammation in acute heart failure.
- Male and female mice equally biosynthesized specialized proresolving mediators; however, female mice generated higher levels of 11,12 epoxyeicosatrienoic acid to coordinate infarct healing after myocardial infarction.

### What Are the Clinical Implications?

- With the current, prevailing view that leukocyte density drives the inflammatory response, the presented outcome supports the concept that resolution (safe clearance of inflammation) is an active process that coincides with the acute inflammatory phase of cardiac repair.
- Men and women are treated using similar therapeutic strategies in cardiovascular medicine, and the measurement of sex-specific bioactive lipid mediators may serve as predictive or prognostic and precise molecular and cellular markers for novel sex-specific therapeutic strategies in patients.

## Nonstandard Abbreviations and Acronyms

<b>AHF</b>	acute heart failure
<b>ALOX-12</b>	lipoxygenase 12
<b>ALOX-15</b>	lipoxygenase 15
<b>ALOX-5</b>	lipoxygenase 5
<b>ALX/FPR2</b>	lipoxin A <sub>4</sub> receptor; formyl peptide receptor
<b>CHF</b>	chronic heart failure
<b>COX-1</b>	cyclooxygenase 1
<b>COX-2</b>	cyclooxygenase 2
<b>DHA</b>	docosahexaenoic acid
<b>EET</b>	epoxyeicosatrienoic acid
<b>HF</b>	heart failure
<b>LV</b>	left ventricle
<b>LXB<sub>4</sub></b>	lipoxin B <sub>4</sub>
<b>MI</b>	myocardial infarction
<b>SPMs</b>	specialized proresolving mediators (ie, lipoxin, resolvins, maresins, and protectin families)

In response to cardiac injuries, such as MI, the leukocyte-directed initiation of inflammation and activation of resolution programs facilitate the clearance and repair of damage myocardium.<sup>12</sup> Delayed initiation of inflammation or immune suppression causes the late arrival of leukocytes to the site of infarction and prolonged residual time of leukocytes during the clearance process; when polymorphonuclear neutrophils are not cleared on time, it can lead to increased, chronic inflammation.<sup>13–15</sup> After experimentally inducing MI by coronary ligation, leukocytes biosynthesize endogenous specialized proresolving mediators (SPMs) that are essential for cardiac healing and repair.<sup>12,16</sup> SPMs are lipoxygenase-mediated omega 3 fatty acid derived biomolecules, including maresins, protectins, resolvins, and lipoxins, that have been shown to have a feed-forward effect on the adaptive immune system, leading to potential therapeutic uses to control inflammation and alleviate chronic diseases.<sup>14,17,18</sup> A positive-feedback loop between SPMs and leukocytes encourages the resolution of injury-induced inflammation by increasing differential lipoxygenase activity.<sup>19</sup> Differences in SPMs between men and women are still being uncovered; therefore, we propose to investigate the differences of cardiac healing in male and female mice with major emphasis on leukocyte trafficking, endogenous bioactive lipid mediators (including SPMs), heart structure, function, and post-MI survival in acute heart failure (AHF) and chronic heart failure (CHF). In the presented report, we aim to explain the differences of male and female C57BL/6J mice in 3 key aspects: (1) the signaling of lipoxygenases and/or cyclooxygenases; (2) the biosynthesis of SPMs in regard to cardiac healing and repair; and (3) cardiac healing in the context of physiological inflammation and resolution response. Our report suggests that male and female mice operate cardiac repair with the biosynthesis of SPMs differently. Male mice have increased overall SPM levels, and female mice have amplified epoxyeicosatrienoic acids (EETs) in AHF with increased levels of reparative macrophages.

## METHODS

Data presented in this article support the findings of this study and are available from the corresponding author on reasonable request.

### Animal Compliance

All animal procedures were conducted according to the National Institutes of Health *Guide for the Care and Use of Laboratory Animals* (eighth edition, 2011) and were approved by the Institutional Animal Care and Use Committees of University of South

Florida (Tampa, FL) and University of Alabama at Birmingham.

### High-Resolution Transthoracic Echocardiography

In vivo cardiac performance of mice was assessed using high-resolution noninvasive echocardiography (Vevo 3100; VisualSonics, Canada) during which mice were anesthetized using a 1-2% isoflurane and 100% oxygen mixture, administered with a small rodent respirator. Body hair on the dorsal side of each animal was removed using depilatory cream at least an hour before the imaging (Nair). Echocardiographic measurement of cardiac structure and function was performed with the high-resolution echocardiography analysis system Vevo 3100 equipped with MX 400 transducer (30 MHz) for small animals. Each measurement was done by a single trained technician (A.B.P.) to eliminate interpersonal variation. Two-dimensional B-mode short-axis and long-axis views, along with B-mode tracings of the left ventricle (LV), were obtained. Using analysis software provided by the manufacturer, the following data were obtained: LV dimension at systole and diastole, posterior wall thickness at systole and diastole, interventricular septal wall thickness at systole and diastole, LV volume at systole and diastole, LV stroke volume, ejection fraction, fractional shortening, heart rate, cardiac output, global longitudinal and global circumferential strain, and LV mass. In addition, the integrated monitoring system allowed measurement of physiological parameters, such as body temperature, ECG, heart rate, and respiration, to be captured and monitored throughout an imaging session.<sup>20</sup>

### Coronary Ligation Microsurgery to Induce MI and Irreversible HF

The hair on the dorsal side of the animal was removed before the surgery. Mice were anesthetized with a 2% isoflurane and 100% oxygen mixture and secured to the operating table. The MI was induced in the mice via ligation of the left anterior descending artery using minimally invasive surgery, as previously described.<sup>21</sup> A total number of 71 mice were subjected to this surgery.<sup>20</sup>

### Measurement of Post-MI Survival

After coronary ligation, mice were monitored closely for recovery and survival monitor and classified into 3 categories. Perioperative mortalities included animals that died during surgery or within the first 24 hours after surgery. Mice that survived 24 hours after surgery but died within 7 days were included within the AHF survival curve. Mice that survived at least 8 days after surgery but died before day (d) 56 were considered in

the CHF survival curve. A necropsy was performed on the mice that died after 24 hours to determine if the mortality was caused by a rupture of the LV or by CHF. Ruptures included all mice with a tear or hole on the LV, resulting in clotted blood within the chest cavity. CHF deaths included mice with no apparent tear or clotted blood in the chest cavity.<sup>4,20,22</sup>

### Necropsy

Animals were anesthetized using a 2% isoflurane and 100% oxygen mixture. From each animal, the LV, lungs, spleen, and tibia were collected. The harvested tissues were either flash frozen and stored at  $-70^{\circ}\text{C}$  and used for Reverse transcription polymerase chain reaction and/or Western blot analysis or placed in 10% zinc formalin and transferred to 70% ethanol after 24 hours and used for histological analysis. The right ventricle was removed from the LV and weighed. The LV was then separated into 3 pieces: the infarct area (infarcted LV [LVI]) or ischemic area below the ligation, the middle piece or the area that has both infarct and remote areas, and the remote area (remote LV) or the area not yet severely affected by the ligation. The ischemic area of the LV and a portion of the spleen were used for gene expression and histological analysis and compared with naïve controls. The lungs are weighed and then placed in an incubator ( $37^{\circ}\text{C}$ ) for 24 hours, and dry weight is recorded.<sup>20</sup>

### Histological Analysis: Hematoxylin and Eosin Staining

Sections of the LV at No-myocardial infarction (MI), MI-d1, and MI-d56 were stained using hematoxylin and eosin, and images were acquired using a BX43 microscope with an attached Olympus DP73 camera, as previously described.<sup>20</sup>

### Confocal Microscopy for Fibrotic Remodeling

For immunofluorescence, sections of the LV at MI-d5 were stained using  $\alpha$  smooth muscle actin, discoidin domain receptor 2, and Hoechst; and confocal images were acquired using a Nikon A1 high-resolution microscope, as described previously.<sup>23</sup>

### Leukocyte Quantitation Using Flow Cytometry

The LV and spleen of No-MI (d0), MI-d1, MI-d3, and MI-d56 male and female mice were taken; and mononuclear cells from both were isolated using methods as previously described.<sup>24</sup> After adjusting for  $\approx 1$  to 2 million cells/stain, the cells were suspended in

100  $\mu$ L of FC block and allowed to incubate for 10 minutes on ice. A stain cocktail containing fluorophore-labeled monoclonal antibodies in 2 $\times$  concentration was added on ice for 30 minutes. The stain cocktail contained CD45-PE-CY7 (BD Biosciences, San Jose, CA), CD11b-APC, F4/80-PERCP (Molecular Probes, Eugene, OR), Ly6C-FITC (BD Biosciences), Ly6G-Pacific blue (e-Bioscience), and LIVE/DEAD Fixable Blue Dead Cell Stain Kit and was used to determine viability and cell type (Figure S1A; gating strategy).<sup>12,25</sup>

### Quantitative Real-Time Polymerase Chain Reaction of Gene Transcripts

RNA was isolated from both the LV and spleen of day 0 (d0) and MI-day 1 (MI-d1) male and female mice. Reverse transcription was performed with 2.0  $\mu$ g of RNA using the SuperScript VILO cDNA Synthesis Kit (Invitrogen, CA). The gene expression levels of *COX-1*, *COX-2*, *ALOX-5*, *ALOX-12*, *ALOX-15*, *IL-1 $\beta$* , *TNF- $\alpha$* , *Arg-1*, *Mrc-1*, *ALX/FPR2*, *EP2*, *EP4*, and *EPHX-2* were measured using TaqMan Probes (Applied Biosystems, CA). The expressions were normalized using hypoxanthine phosphoribosyltransferase 1 (*HPRT1*). The results were reported using  $2^{-\Delta\text{Ct}}$  values.<sup>20</sup>

### Protein Extraction and Immunoblotting

Protein was extracted from the LVI or the remote LV, as previously described.<sup>26</sup> After electrophoresis of 5 to 10  $\mu$ g of LVI or remote LV protein, primary antibodies *ALOX-5*, *HO-1*, *COX-2*, *ALX/FPR2*, *TNF- $\alpha$* , or *GAPDH* were allowed to incubate overnight at 4°C. After the incubation, respective secondary antibody (1:10 000 dilution in a 5% blocking solution) was added, as previously described.<sup>26</sup> Femto chemiluminescence detection system was used to detect protein expressions (Pierce Chemical, Rockford, IL). To normalize the total protein/lane, densitometry was performed using Image J software (NIH, Bethesda, MD).<sup>26</sup>

### Quantification of SPMs Using Mass Spectrometry

Samples of the LV and spleen for liquid chromatography–tandem mass spectrometry analysis were obtained using solid phase extraction columns, as described.<sup>12</sup> To observe and measure the levels of lipid mediators in the LVI, an LC-tandem MS/MS system, QTrap 5500 (ABSciex), equipped with an Agilent HP1100 binary pump, was used. The Agilent Eclipse Plus C18 column (50 mm $\times$ 4.6 mm $\times$ 1.8  $\mu$ m or 100 mm $\times$ 4.6 mm $\times$ 1.8  $\mu$ m) with a gradient of methanol/double-distilled H<sub>2</sub>O/acetic acid (60:40:0.001 to 100:0:0.01) was used at a flow rate of 0.5 mL/min. If

a standard for a product was not available, a product with similar chromatographic behaviors was used for a calibration curve. Deuterium-labeled internal standards included lipoxin A<sub>4</sub>, resolvin D1 (RvD1), Prostaglandin E<sub>2</sub> (PGE<sub>2</sub>), leukotriene B<sub>4</sub>, and others, obtained from Cayman Chemical Company (Ann Arbor, MI) and used to calculate recoveries. The peak area of each Multiple Reaction Monitoring (MRM) transition and linear calibration curves were used for the quantification of each mediator.<sup>27</sup> A minimum of 6 characteristics and diagnostic ions were used for identification of all SPMs, in accordance with published criteria of biologic and synthetic mediators.<sup>27,28</sup>

### Statistical Analysis

The results are expressed as mean $\pm$ SEM. Analyses were performed using a 2-way ANOVA (mixed model); multiple comparisons are done using Sidak test recommended parameter for time kinetics and post Tukey test for other comparisons (Graphpad Prism 8.3.0 application). The Kaplan-Meier test and log-rank test were followed for survival analysis.  $P < 0.05$  was considered as statistically significant.

## RESULTS

### Female Mice Have Higher Survival With Few Ruptures in AHF

To determine the sex-specific differences between male and female mice after permanent coronary ligation, we measured long-term survival, cardiac function, myocardium structural integrity, and gene and protein expression (Figure 1A: study design). A total of 43 male mice and 28 female mice were subjected to occlusion of the left anterior descending coronary artery. Successful MI and LV dilation were confirmed using echocardiography within 24 hours after surgery with the inclusion criteria of fractional shortening <15%. Any mortalities within the first 24 hours were considered perioperative mortalities and excluded from the survival curve ( $\approx$ 5% for the trained surgeon). After analyzing the mortality rate of the mice after MI using Kaplan-Meier curve, we separated the deaths into either AHF (MI-d1 to MI-d7) or CHF (MI-d8 to MI-d56). Deaths in these categories were further divided into HF or ruptures. In response to coronary ligation, the overall survival in female mice is 21% higher compared with male mice, without developing CHF or a rupture up to 56 days after MI (Figure 1B and 1C). A breakdown of the survival chart into the short- and long-term phases shows that male mice have increased mortality attributable to ruptures (28% compared with 7% in female mice) and CHF (12% compared with 7% in female mice)

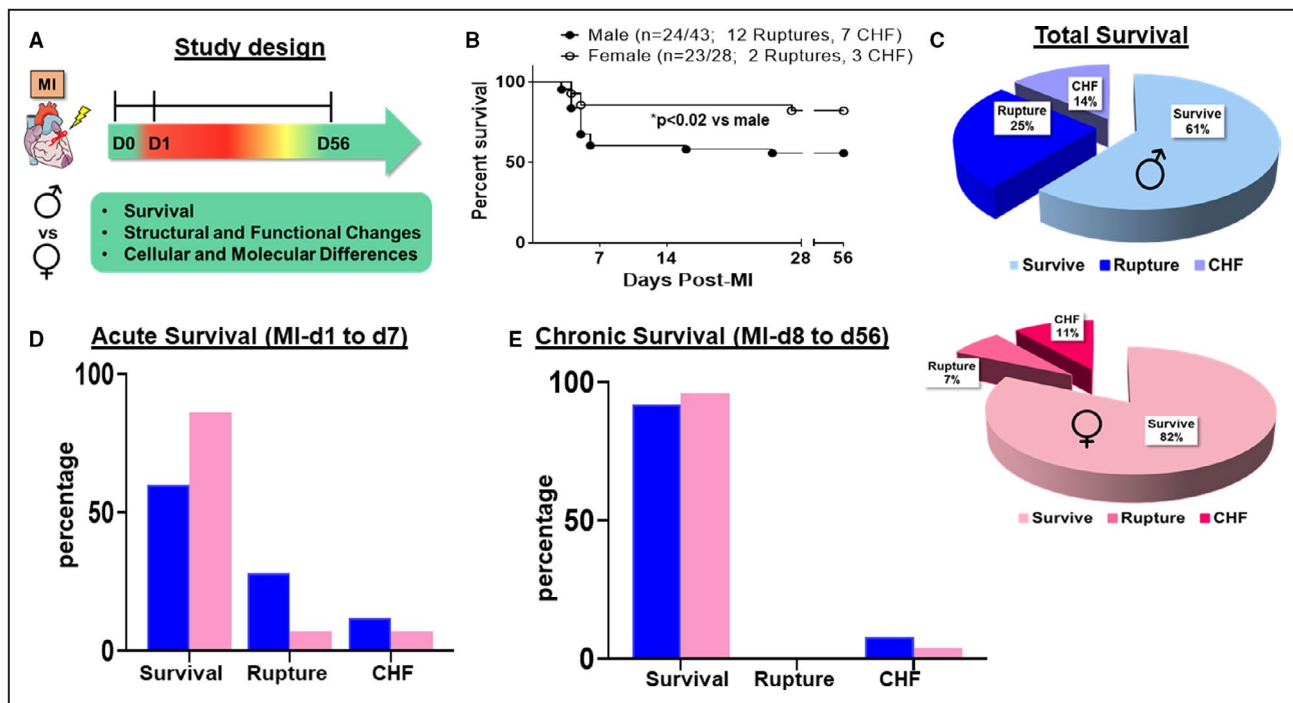


**Figure 1.** Female mice have higher survival than male mice without ruptures or chronic heart failure (CHF) after myocardial infarction (MI).

**A**, Study design to evaluate differences in male and female C57BL/6J mice after MI in acute heart failure (AHF) and CHF induced by left anterior descending artery ligation. **B**, Survival rates of both sexes using the Kaplan-Meier test in AHF and CHF. **C**, Pie chart showing the survival rates of both sexes. **D** and **E**, Bar graph showing the survival rates of both sexes in AHF and CHF. Males (n=43), females (n=28). \*P<0.02 vs male analyzed by log-rank test.

within 7 days of MI (Figure 1D; Figure S1B). Within the long-term phase (after MI-d7), there is no significant difference in either rupture or CHF mortalities between male and female mice (Figure 1E; Figure S1C). This in-depth survival analysis allowed for the more accurate differentiation between male and female survival after MI and pinpointed the sex-specific responses to AHF and CHF.

### Female Mice Show Improved Recovery and Heart Function After MI

Gravimetric parameters were measured to more accurately rule out variables between male and female mice (Table 1). After the coronary ligation surgery, echocardiograms of both male and female mice showed reduced cardiac function consistent with HF (Figure 2). In both sexes, LV dilation was evident by the decrease in vector length (longitudinal and circumferential axis b-modes), increased strain on the myocardium (strain), and myocardium dyssynchronicity (segmental synchronicity) of the representatives for MI-d1 to MI-d56 compared with the No-MI controls (Figure 2). However, after an initial decrease, female mice recovered a portion of their cardiac function at MI-d3, which continued to gradually increase until MI-d56, shown by increased vector length (longitudinal

and circumferential axis b-modes), decreased muscle strain (strength), and improved synchronicity (segmental synchronicity) (Figure 2). The improvement of the female mice heart function is further shown by the increase in their fractional shortening (MI-d56: 19% in females compared with 8% in males) and global longitudinal strain (MI-d56: -11% in females compared with -6% in males) (Table). Thus, improvement in heart functional recovery is believed to be enabling the female mice to “bounce back” and survive at a significantly higher rate than male mice after MI.

### Cardiac Tissue Repair Marked With SPM Biosynthesis With Higher Levels of EETs in Female Mice

After discovering the higher survival in females is caused by lower rupture rates in AHF, we quantified the levels of proinflammatory mediators, endogenous SPMs, and EETs in the LVI at d1 after MI (Figure 3A through 3F and Figure S2). The arachidonic acid-derived proinflammatory mediators, such as leukotriene B<sub>4</sub>, Prostaglandin (PG)D<sub>2</sub>, PGE<sub>2</sub>, PGF<sub>2</sub>α, and Thromboxane B<sub>2</sub> (TXB<sub>2</sub>), were increased in both male and female mice as signs of initiation of an inflammatory response (Figure S3) and simultaneous biosynthesis of SPMs as resolving response (Figure S4). The

**Table. Echocardiography and Necropsy Parameters for Male and Female Mice at MI-d1, MI-d3, MI-d5, and MI-d56 Compared With Naive Controls.**

Echocardiographic Parameters	No-MI Controls		MI-d1		MI-d3		MI-d5		MI-d56	
	Male (n=18)	Female (n=18)	Male (n=19)	Female (n=19)	Male (n=5)	Female (n=5)	Male (n=6)	Female (n=6)	Male (n=14)	Female (n=12)
Heart rate, bpm	484±7	475±6	525±17	500±13	568±27	522±26	571±20	529±13	487±14	439±24
EDD, mm	4±0.09	4±0.08	4±0.09	4±0.07	5±0.19	4±0.09	5±0.30	4±0.22	6±0.18*	4±0.14†
ESD, mm	3±0.11	2±0.08	4±0.12*	3±0.11*	4±0.18*	3±0.07†	4±0.33*	3±0.27†	6±0.16*	3±0.25†
Fractional shortening, %	36±2	35±1	10±1*	13±2†	13±3*	15±1†	11±2*	18±3†	5±0.5*	22±4†
IVSd, mm	0.82±0.04	0.93±0.05	0.71±0.07*	0.70±0.05*	0.62±0.08*	0.84±0.09†	0.61±0.05*	0.64±0.07*	0.29±0.02*	0.70±0.10†
PWTd, mm	0.75±0.02	0.78±0.04	0.64±0.04*	0.66±0.04*	0.68±0.07*	0.65±0.04*	0.56±0.04*	0.64±0.08†	0.31±0.03*	0.80±0.09†
IVSs, mm	1.16±0.05	1.16±0.07	0.82±0.08*	0.78±0.05†	0.81±0.05*	0.92±0.14†	0.78±0.07*	0.96±0.10†	0.36±0.05*	0.91±0.15†
PWTs, mm	1.06±0.06	0.99±0.03	0.74±0.05*	0.80±0.06†	0.80±0.05*	0.81±0.06*	0.57±0.03*	0.85±0.07†	0.36±0.03*	1.07±0.13†
GLS	-20±1	-20±1	-7±1*	-8±1*	-10±1*	-12±2†	-7±1*	-12±2†	-4±0.4*	-13±2†
Necropsy parameters										
Body weight, g	26±1	22±1	26±1	22±1	27±1	24±2	29±1	24±2	31±1	28±1
LV, mg	98±7	80±2	100±2*	74±2†	121±8*	92±5†	128±3*	99±6†	113±4*	83±3†
LV/BW, mg/g	4±0.2	4±0.1	4±0.1	3±0.1	4±0.2	4±0.2	4±0.1	4±0.3	4±0.1	3±0.1
RV, mg	18±0.7	14±0.6	16±0.4	15±1	21±2	15±2	23±1*	18±1	22±2*	15±1
Spleen, mg	89±3	86±2	70±2	72±3	106±5*	109±9*	109±10*	99±11*	79±3	85±3
RV mass/BW, mg/mg	0.7±0.03	0.6±0.03	0.6±0.02	0.7±0.03	0.8±0.05	0.7±0.4	0.8±0.04	0.8±0.05	0.7±0.05	0.6±0.03
Lung mass/BW, mg/mg	7±0.6	7±0.5	7±0.3	7±0.3	7±0.4	9±1	8±2	8±1	5±0.3	6±0.6
Tibia, mm	15±0.2	15±0.2	15±0.2	15±0.2	17±0.2	16±0.4	17±0.1	16±0.2	17±0.2	16±0.3

Data are given as mean±SEM. Bpm indicates beats per minute; BW, body weight; EDD, end diastolic dimension; ESD, end systolic dimension; GLS, global longitudinal strain; IVSd, intraventricular septum diastole; IVSs, intraventricular septum systole; LV, left ventricle; PWTd, posterior wall thickness diastole; PWTs, posterior wall thickness systole; RV, right ventricle; MI, myocardial infarction; and day, d.

\*P<0.05 vs No-MI naive controls.

†P<0.05 vs male mice at respective time point.

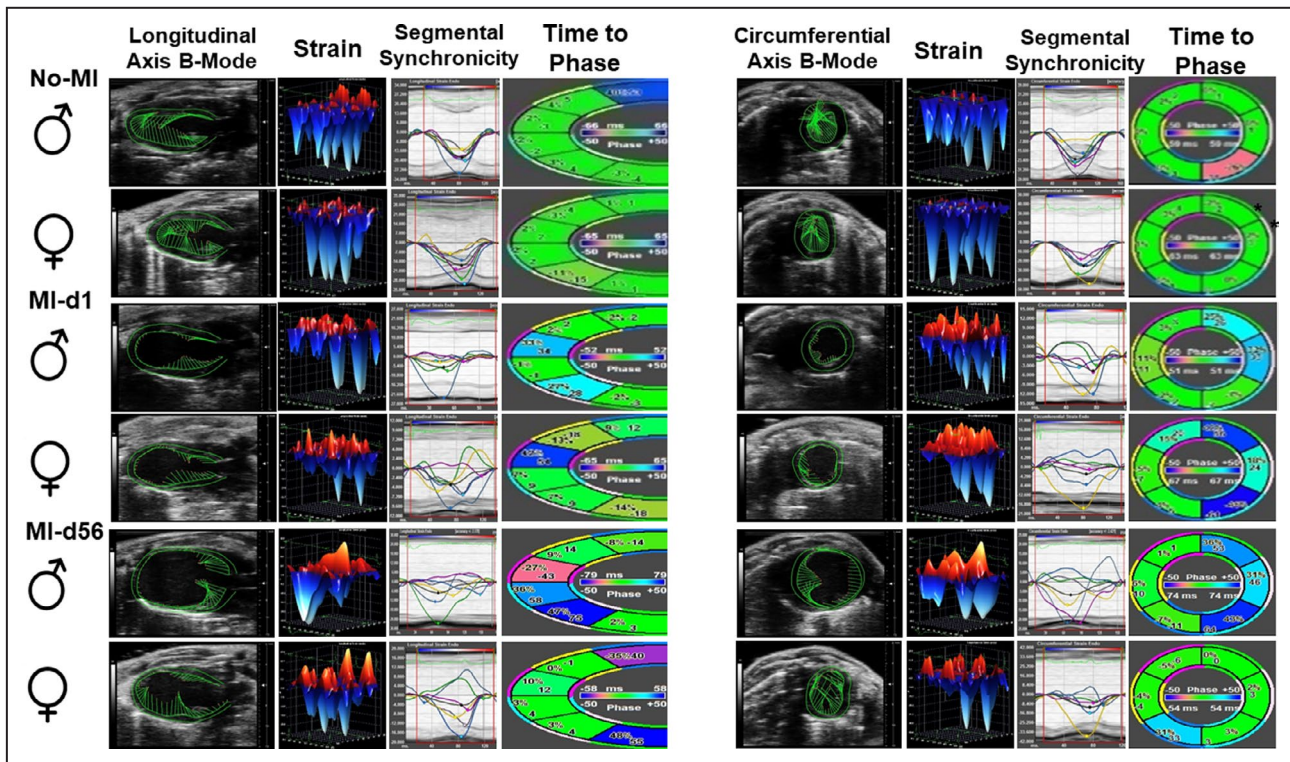


**Figure 2. Female mice show better recovery of function and synchronicity from MI-d1 to MI-d56.** Speckle tracking-based echocardiography representatives of male and female mice at No-MI, MI-d1, and MI-d56 (from left: longitudinal axis 2-dimensional [2D] B-mode, longitudinal 3-dimensional [3D] strain, longitudinal segmental synchronicity graph with displayed curves, and longitudinal time to phase; short axis 2D B-mode, circumferential 3D strain, circumferential segmental synchronicity graph with displayed curves, and circumferential time to phase). Males (n=5-18), females (n=5-19).

pie chart distribution of SPMs reflects high SPM cluster in male mice (17%) compared with female mice (11%) in LVI (Figure 3C and 3D). The individual quantification of D-series resolvins, maresins, protectins, and arachidonic acid-derived SPMs suggests male and female mice biosynthesis of SPMs with activation of proinflammatory mediators, suggestive of overlapping inflammation-resolution response in cardiac repair (Figure 3A through 3E). The female mice have higher levels of p450-mediated arachidonic acid-derived EET compared with the male counterparts, specifically a significant (1.3 fold;  $P < 0.05$ ) increase in 11,12-EETs (Figure 3F). The quantitative analyses of endogenous bioactive lipids suggest that despite similar SPM contributions in cardiac repair, females have the tendency to produce higher levels of arachidonic acid-derived cypoxins (EETs) compared with the males in infarcted LV in AHF after MI.

### Differential Lipoxygenase and Cyclooxygenase Activation in Male and Female Mice in AHF

After myocardium injury, cyclooxygenase (COX-1 and COX-2) and arachidonate lipoxygenase (ALOX-5,

ALOX-12, and ALOX-15) activity increases at the site of infarction. To determine the differences in initiation of inflammation-resolution between male and female mice, the expression of cyclooxygenases and lipoxygenases was quantified from the spleen and LV for the following time points: No-MI, MI-d1, and MI-d56 (Figure 4A through 4M). At MI-d1, ALOX-5 had higher expression in the male spleen compared with females (Figure 4A). In response to cardiac injury, immune responsive lipoxygenases (5, 12, and 15) and cyclooxygenases (1 and 2) are amplified at MI-d1 in both the LV and spleen as signs of inflammatory and beginning of resolution signal for the biosynthesis of SPMs (Figure 4A through 4J). Female splenic and LVI expressions of COX-1 are higher than male expression at MI-d1 (Figure 4G and 4I). Expression of COX-2 showed no difference between the males and females (Figure 4H and 4J). The expression levels of lipoxygenases and cyclooxygenases in the spleen and LV of male and female mice returned to the normal, homeostatic levels at MI-d56 as a signal of physiological control and resolved inflammation (Figure 4A through 4J). LV protein levels show male mice produce more ALOX-5 and COX-2 at MI-d1 compared with female mice (Figure 4K through 4M). These results indicate the spleen and

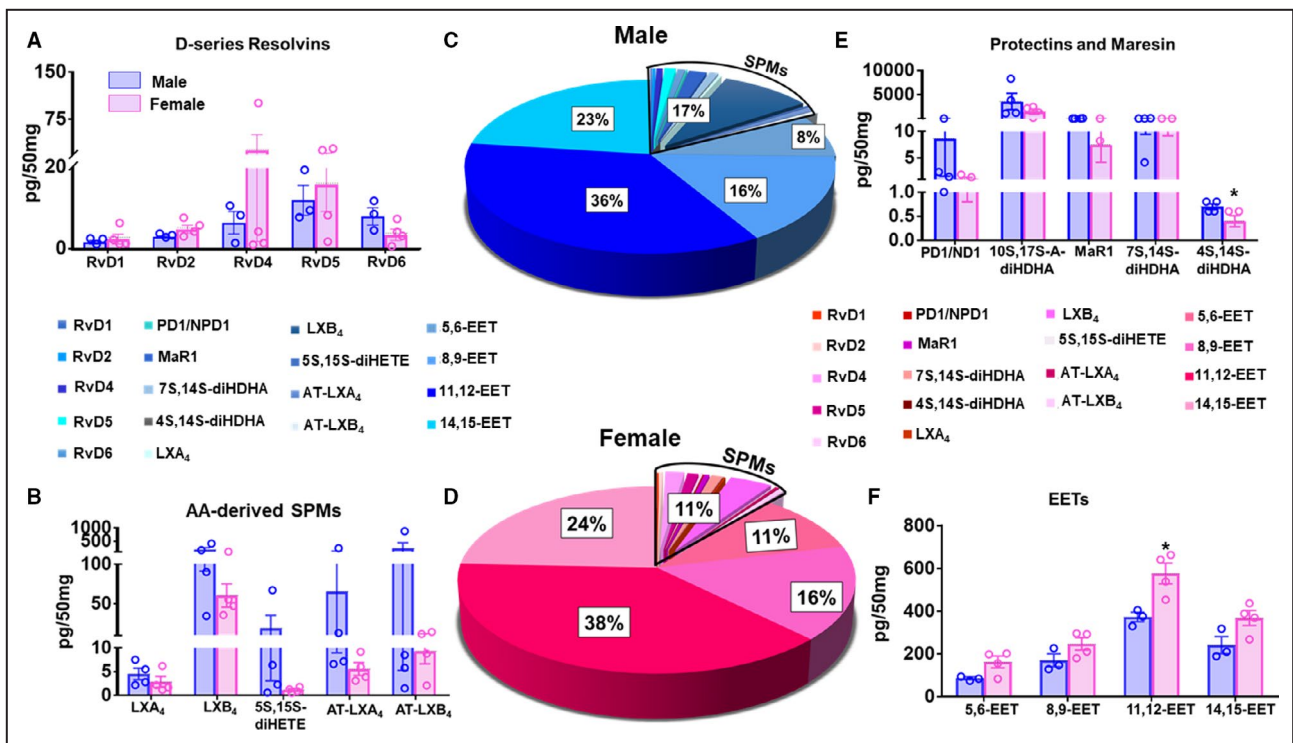


**Figure 3. Both sexes biosynthesized similar amounts of specialized proresolving mediators (SPMs) after cardiac injury.** **A**, Bar graph showing the docosahexaenoic acid (DHA) series resolvins of the left ventricle at myocardial infarction (MI)-day (d1 of male and female mice. **B**, Bar graph showing the arachidonic acid (AA)-derived SPM moieties of the left ventricle at MI-d1 of male and female mice. **C**, Pie chart showing the SPMs (resolvins, protectins, maresins), epoxyeicosatrienoic acids (EETs), and AA-derived SPMs in the left ventricle of male mice at MI-d1. **D**, Pie chart showing the SPMs (resolvins, protectins, maresins), EETs, and AA-derived SPMs in the left ventricle of female mice at MI-d1. **E**, Bar graph showing the protectins and maresins of the left ventricle at MI-d1 of male and female mice. **F**, Bar graph showing the EETs of the left ventricle at MI-d1 of male and female mice (MI-d1: males [n=3], females [n=4]). \*P<0.05 vs male MI-d1.

infarcted heart coordinate endogenous biosynthesis of lipid mediators in cardiac repair during acute myocardial injury.

### Distinct Reparative Structural Remodeling in Female Mice in AHF

Adverse myocardium structural remodeling is a primary risk factor for CHF after MI. To define recovery, we examined hematoxylin and eosin stained LV sections at No-MI controls, MI-d1, and MI-d56 (Figure 5A). For each MI time point, we examined the remote (noninfarcted area after MI), peri-infarct (the area between the remote and infarct), and the infarct (thin-wall area of the myocardium) areas to get an accurate representation of the progression of cell apoptosis and cardiac repair. The remote areas at the No-MI and MI-d1 time points of both the male and female mice show parallel cardiomyocyte, elongate, and centrally located nuclei and intercalated disks in myocardium structure (Figure 5A). However, at MI-d56, the tissue damage has expanded to the remote area and the peri-infarct and infarct areas, with persistent scar within the myocardium structure, and the non-myocyte nuclei are misplaced and are congregated

within the dead tissue, decreasing structural integrity and aligning with the CHF phenotype (Figure 5A). No difference was observed in the cardiomyocyte area between male and female mice (Figure S5). Fibrotic remodeling further confirmed by a smooth muscle actin and discoidin domain receptor 2 staining to determine fibroblast activation and presence of collagen in AHF at MI-d5 (Figure 5B). The female LVI showed lower expression of  $\alpha$  smooth muscle actin and discoidin domain receptor 2 compared with male LVI, indicating limited fibrotic remodeling (Figure 5B). Thus, limited fibrotic and structural remodeling in female mice supports the improved functional recovery and survival in both AHF and CHF.

### Reparative Monocytes Are Higher in Female Mice Compared With Male Mice After MI

Initiation of inflammation in AHF is defined by the entry of leukocytes at the site of injury with continuum phenotype spectrum; therefore, we analyzed how sex-specific differences impacted LV leukocyte populations after MI using flow cytometry during AHF and CHF<sup>24</sup> (Figure S6). At naïve homeostatic setting, male



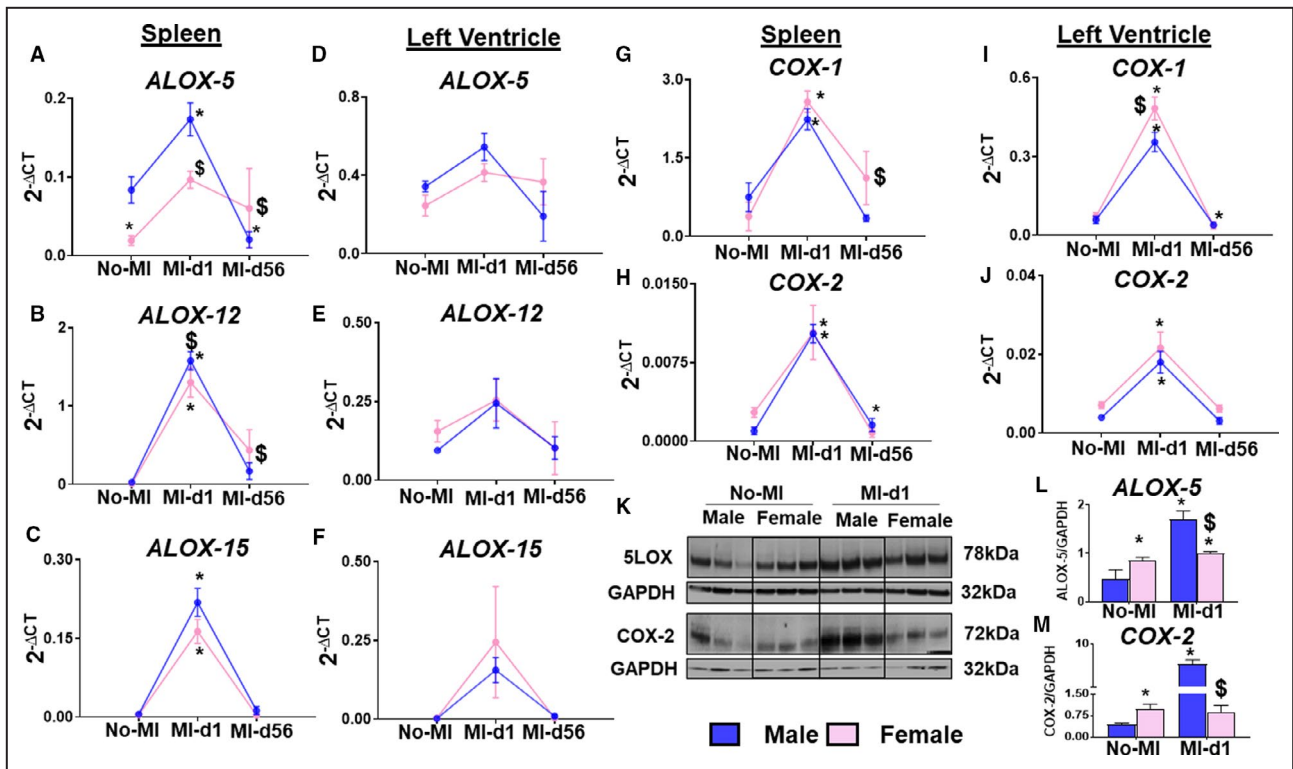


**Figure 4. Male mice have a higher level of lipoxigenase (LOX) expression, whereas female mice express higher cyclooxygenases (COXs) after MI.**

**A through F.** Line graphs of LOXs (*ALOX5*, *ALOX12*, *ALOX15*) in the spleen and left ventricle of male and female mice from No-MI to MI-d1. **G through J.** Bar graphs of COXs (*COX1*, *COX2*) in the left ventricle of male and female mice from No-MI to MI-d1 (no-MI: males [n=4], females [n=4]; MI-d1: males [n=6], females [n=6]). \*P<0.05 vs no-MI naïve controls; §P<0.05 vs male at respective time point. **K through M.** Western blot representative and bar graphs of protein expression of *ALOX5* and *COX2* (n=3/group). \*P<0.05 vs no-MI naïve controls; §P<0.05 vs male at respective time point.

and female mice show no difference in LV monocyte (CD45<sup>+</sup>/CD11b<sup>+</sup>) populations. In response to ischemic insult, male and female monocytes consistently amplified from d1 to d5 after MI. In both male and female mice, monocyte populations declined at d56 (CHF), comparative to pre-MI naïve state. Female mice showed lower monocytes (53±4.3%; P<0.05) when compared with the male mice (68±3.9%) in AHF (after MI-d5) (Figure 6A through 6G). Although, in both male and female mice, monocyte population declined at d56 after MI (CHF), in females, monocyte population was significantly higher (16.0±2.1%) compared with the male counterpart, which displayed (1.6±0.2%) of monocytes (Figure 6A and 6E). However, no sex-specific changes in CD11b<sup>+</sup> expression were observed (Figure 6B). Furthermore, the phenotypic analysis of LV monocytes on basis of Ly6C<sup>lo</sup> and Ly6C<sup>hi</sup> displayed female mice had a higher Ly6C<sup>lo</sup> population (18±0.7%), compared with male mice (14±0.7%) at d1 after MI, which remained significantly higher in CHF (Figure 6C, 6D, 6F, and 6G). Increased reparative monocytes during AHF support the improved cardiac repair, functional recovery, and limited fibrotic remodeling of female mice.

### Female Mice Have Intensified Dendritic Cell Activation in Cardiac Repair Than Male Mice After MI

After the ischemic insult, dendritic cells (DCs) are an essential part of the innate immune leukocyte system. DCs act as a bridge to the adaptive immune system and play a tissue reparative role in cardiac healing, as the inadequate levels of DCs led to increased rupture and impaired reparative fibrosis after MI.<sup>29</sup> In the absence of cardiac injury (No-MI), no difference was observed in CD11c-positive cells between male and female mice (Figure 7A and 7E). In response to coronary ligation, there was a consistent increase in CD11c cells in AHF (MI-d1, MI-d3, MI-d5) and a CD11c<sup>+</sup> cell population decline at CHF (MI-d56), irrespective of sex-specific. At post-MI-d1, female mice displayed a higher percentage of CD11c<sup>+</sup> cells (3.2±0.5%) compared with male mice (1.8±0.2%), and the DC population peaked at d5 and remained significantly higher in females. Compared with AHF, the DC population declined with time in CHF but relatively remained higher in females compared with males (Figure 7A, 7B, and

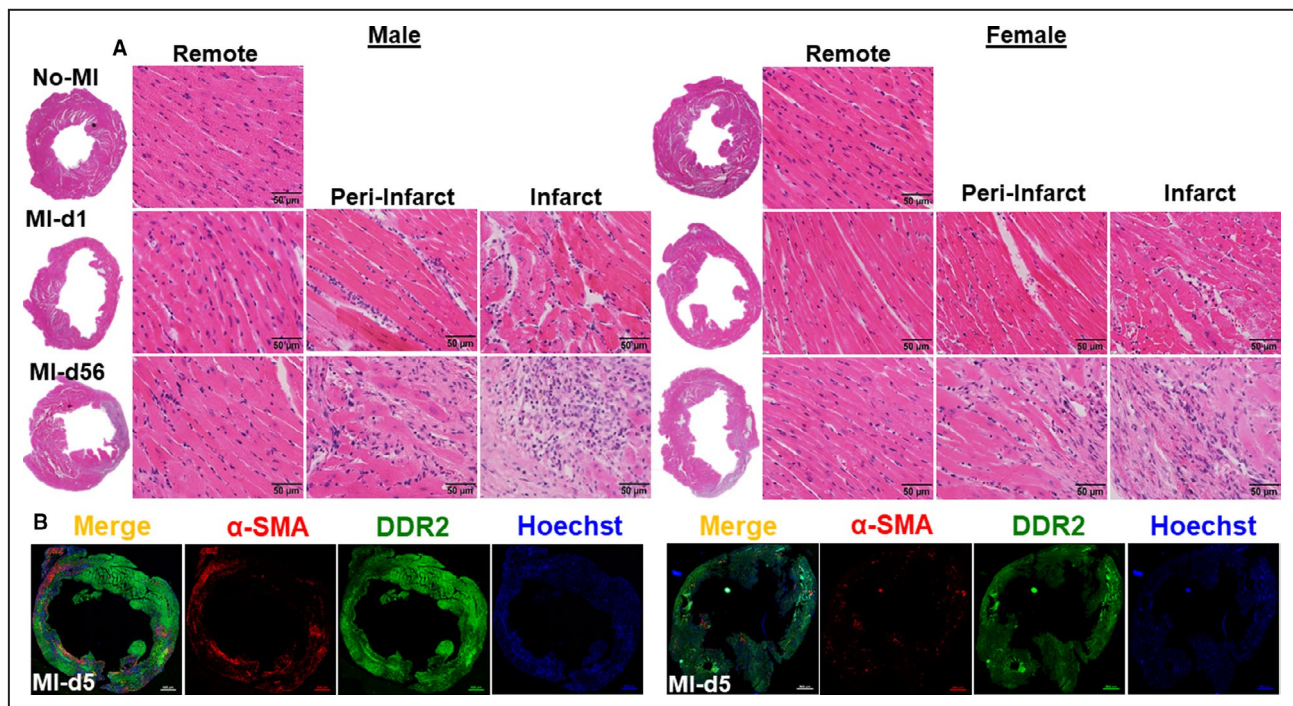


**Figure 5.** Female mice display a lower level of  $\alpha$ -smooth muscle action ( $\alpha$ -SMA) compared with male mice at d5 after MI with similar intensity of remodeling.

**A**, Representative hematoxylin and eosin stained left ventricular (LV) images from d0 naïve control (No-MI); MI-d1 is suggestive of acute heart failure (HF), and MI-d56 is indicative of chronic HF in male and female mice. Representative images of remote (left), peri-infarct (middle), and infarct area (right) with a magnification of  $\times 40$  and accompanying  $\times 1.25$  images ( $n=4-5$  mice/group/day; bar= $50\ \mu\text{m}$ ). **B**, Immunofluorescence images indicating reduced  $\alpha$ -SMA (red) and discoidin domain receptor 2 (DDR2; green) expression in LV of females at d5 after MI. Nuclei are stained with Hoechst (blue) (bar= $500\ \mu\text{m}$ ).

7E). As expected, the neutrophils are the first phagocytic responder in cardiac injury. The quantitative analyses of neutrophil populations from male and female mice showed that neutrophils peaked at post-MI-d3 and reached the homeostatic level at d56 after MI. The percentage neutrophil population showed no statistical difference in male and female mice in the infarcted area (Figure 7C, 7D, and 7F).

Analysis of macrophage kinetics ( $\text{CD45}^+\text{CD11b}^+\text{F4/80}^+$ ) showed a peak at MI-d5, with a decline in their population at MI-d56. However, male and female mice displayed a similar percentage of macrophage populations (Figure S6A through S6E). The macrophages are subclassified as  $\text{Ly6C}^{\text{lo}}$  and  $\text{Ly6C}^{\text{hi}}$ , indicative of their proinflammatory and/or reparative function, so we quantified  $\text{F4/80}^+$  cardiac macrophages after MI by  $\text{Ly6C}^{\text{lo/hi}}$  expression. Males and females equally amplified the  $\text{Ly6C}^{\text{hi}}$  population, but females displayed a higher population of  $\text{Ly6C}^{\text{lo}}$  cells ( $8.5\pm 1.3\%$ ) compared with males ( $1.1\pm 0.1\%$ ) at post-MI-d56, contributing to improved cardiac repair (Figure S6B and S6F). Leukocyte-directed physiological inflammation in the female is marked with activation of reparative monocytes and macrophages, with an amplified density of DCs in short-term cardiac repair with the limited

difference in CHF. This male and female leukocyte diversity suggests physiological cardiac repair in females expedited by the presence of a higher number of DCs and reparative monocytes and macrophages in AHF.

### Female Mice Activate the Inflammation-Resolution Sensor and Cytokines in the LVI After MI

To define cardiac healing in AHF and CHF, the differences in cytokines and the bioactive lipid mediator receptors of male and female mice and the levels of proinflammatory and inflammation controlling cytokines within the spleen and LVI at MI-d1 were measured. The male mice showed increased expression of *TNF- $\alpha$* , *IL-1 $\beta$* , *ARG-1*, and *MRC-1* within the spleen (Figure 8A through 8D); and the female mice showed higher expression of the same cytokines within the LVI at MI-d1 (Figure 8E through 8H). The male mice showed higher protein levels of *TNF- $\alpha$*  in the LVI compared with females, indicating divergence in the levels of RNA and protein (Figure 8I and 8J). Male mice also had increased expression of *HO-1* in the LVI (Figure 8K). Furthermore, we determined receptors (*ALX/FPR2*, *EP2*, and *EP4*) and cypoxins (EETs) metabolizing enzyme (*EPHX2*)

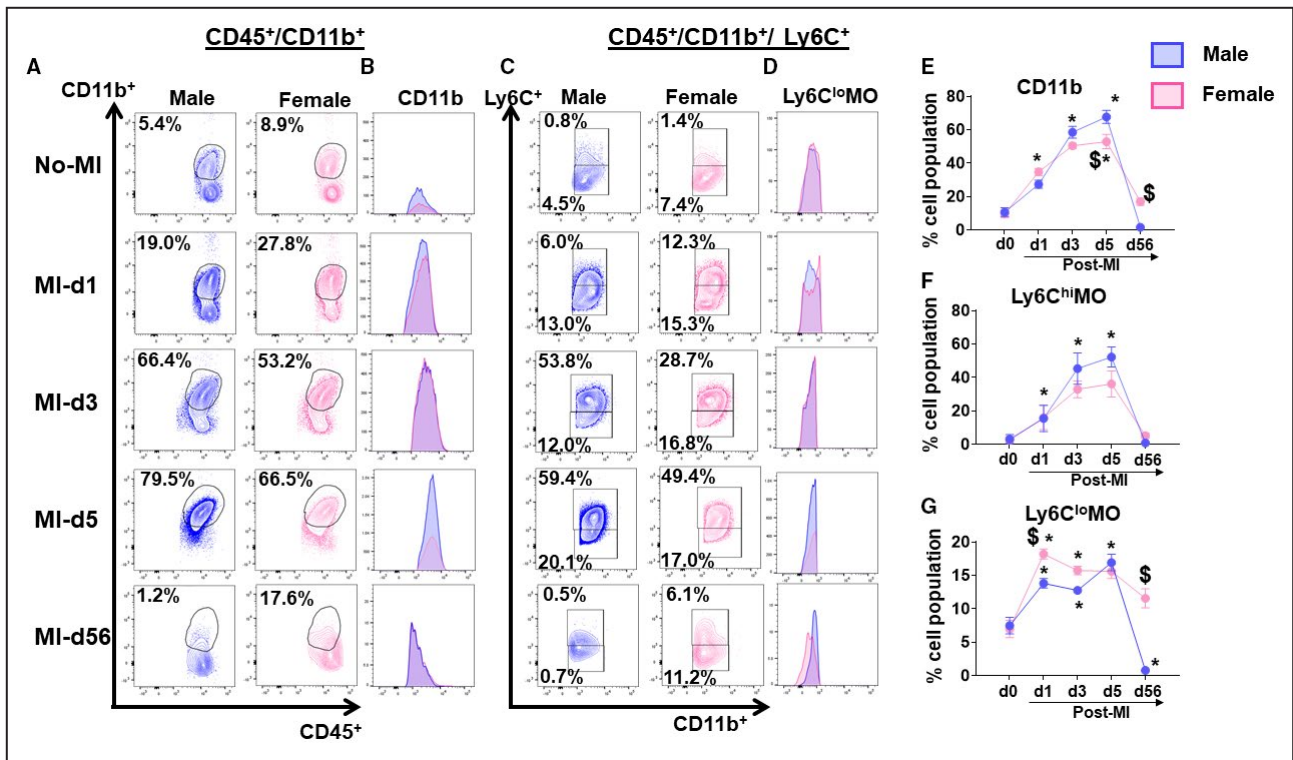


**Figure 6. Female mice show higher reparative monocytes compared with male mice after myocardial infarction (MI).** (A) Plot showing cluster of differentiation (CD)11b<sup>+</sup> (monocytes) cells at No-MI, MI-d3, MI-d5, and MI-d56 in male and female mice. (B) Histograms showing monocytes expression at No-MI, MI-d3, MI-d5, and MI-d56 in male and female mice. (C) Plot showing cluster of Ly6C<sup>hi</sup> and Ly6C<sup>lo</sup> cells at No-MI, MI-d3, MI-d5, and MI-d56 in male and female mice. (D) Histograms showing Ly6C<sup>hi</sup> and Ly6C<sup>lo</sup> monocytes expression at No-MI, MI-d3, MI-d5, and MI-d56 in male and female mice. (E, F, G) Line graphs showing the percentage of the cell population for CD11b, Ly6C<sup>hi</sup> monocytes (MO), and Ly6C<sup>lo</sup>MO. [No-MI: males (n=4), females (n=4); MI-d1: males (n=5), females (n=6); \$P<0.05 vs male at respective time point; \*P<0.05 compared with no-MI naïve controls.

gene expression within the spleen and LVI and found minor sex-specific differences in levels of *ALX/FPR2*, *EP4*, *EP2*, and *EPHX2* within the spleen (Figure 9A through 9D). In infarcted heart, *ALX/FPR2* and *EP4* activation were significant in female mice, suggestive of amplified receptor activation in female mice during cardiac repair (Figure 9E through 9H).

## DISCUSSION

After the ischemic insult, unresolved inflammation-directed HF has increasingly become one of the main causes of death, both within the United States and worldwide; however, the differences in how HF is presented and managed between men and women have been inadequately investigated. The major risk factors for CVD are universal and independent of sex and can include aging, obesity, hypertension, diabetes mellitus, alcohol consumption, and smoking.<sup>9,30</sup> Regardless of this, women are less likely to develop CVD or HF compared with men, unless they are significantly older.<sup>30-32</sup> In addition, hypertension

has a greater impact on men developing HF than women.<sup>30</sup> To define physiological inflammation and cardiac repair in the absence of diversified risk factors, we described leukocyte-directed molecular and cellular differences in male and female mice. Our key findings are as follows: female mice (1) have higher survival and lower rupture rates; (2) have amplified reparative monocytes, DCs, and macrophages; and (3) produced higher levels of EETs compared with male mice during the cardiac repair. Our functional and molecular analysis provides understanding about the difference between male and female mice in cardiac repair (Figure 9I).

Differences in cardiovascular morbidity and mortality caused by sex have not been adequately researched. Most mortalities develop with age, and several reports have only studied young mice in this context. Therefore, studies on phenotypical determinations need to balance sex ratios to avoid misleading information when a sex difference does exist. Our study showed the overall survival after MI is higher in female mice compared with male mice, which is in accordance with humans, where women have a

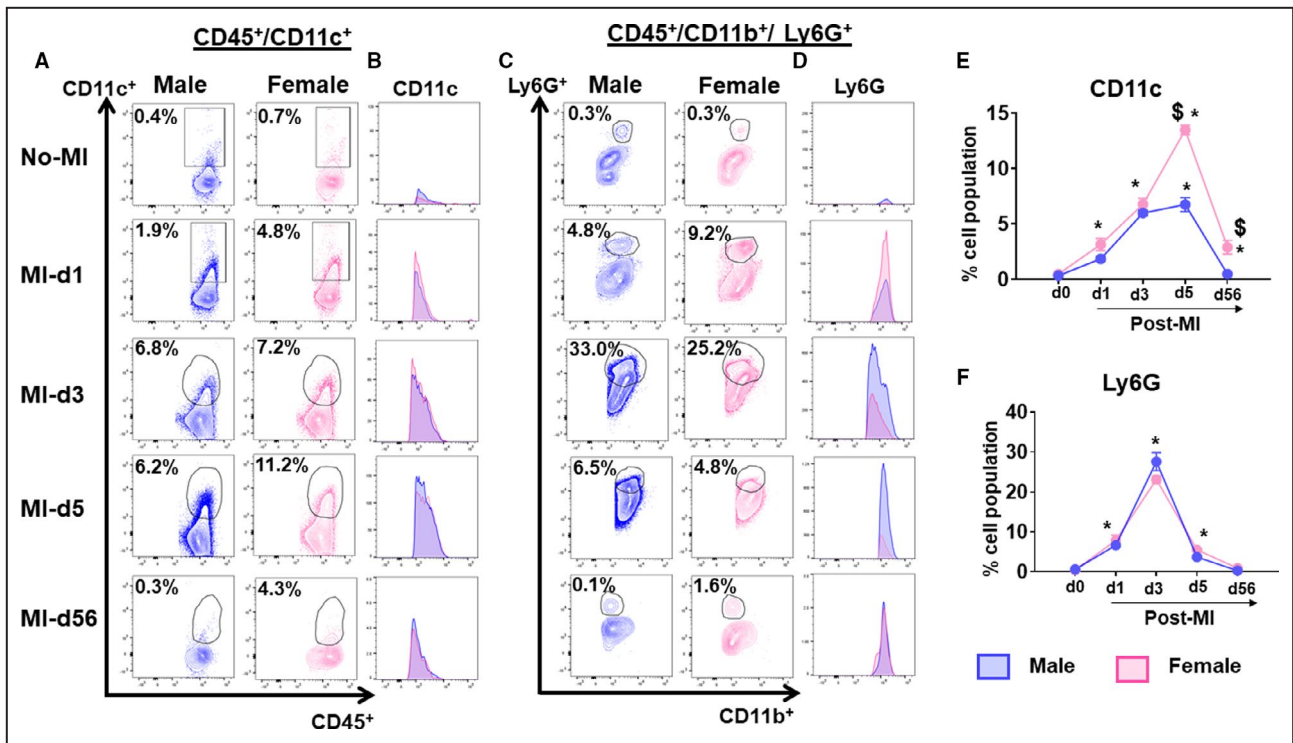


**Figure 7. Female mice intensified leukocyte response compared with male mice after myocardial infarction (MI).** (A) Plot showing dendritic cells (CD11c<sup>+</sup>) at No-MI, MI-d3, MI-d5, and MI-d56 in male and female mice. (B) Histograms showing dendritic cells at No-MI, MI-d3, MI-d5 and MI-d56 in male and female mice. (C) Plot showing neutrophils (Ly6G<sup>+</sup>) at No-MI, MI-d3, MI-d5, and MI-d56 in male and female mice. (D) Histograms showing neutrophils expression at No-MI, MI-d3, MI-d5 and MI-d56 in male and female mice. (E, F, G) Line graphs showing the percentage of the cell population of CD11c and Ly6G. [No-MI: males (n=4), females (n=4); MI-d1: males (n=5), females (n=6); <sup>§</sup>P<0.05 vs male at respective time point; \*P<0.05 compared with no-MI naïve controls.

lower risk for HF than men.<sup>31,33</sup> It was well noted that major differences in the survival rates between the male and female mice occur during AHF, whereas both male and female mice showed no difference in survival rates during CHF. This study showed female mice having a rupture rate of 7%, whereas in male mice, rupture rates were 28% in AHF. In recent decades, research on sex-related differences in cardiovascular medicine has been focused on demonstrating the role of hormones, but leukocyte phenotypes and their population differences caused by sex remained understudied.

The post-MI leukocyte-derived growth factors, cytokines, and different mediators are major contributors to inflammation and resolution. Moreover, leukocyte populations differ considerably within male and female mice during clot formation and AHF.<sup>12,34,35</sup> Female mice showed higher population of reparative monocytes and macrophages (Ly6C<sup>lo</sup> monocytes and Ly6C<sup>lo</sup> macrophages), indicative of healing response.<sup>12,36</sup> Studies have demonstrated that DC numbers increase in infarcted hearts of experimental models,<sup>37</sup> and decreased numbers of DCs in human infarcted myocardial tissue are associated with impaired reparative fibrosis and the development of cardiac ruptures after MI.<sup>29</sup>

Female mice not only displayed high DC populations at both AHF and CHF, which provides early inflammation-resolution benefits and plays a role in fibrotic repair. DC infiltration in human infarcted myocardium showed a strong association between the number of DCs and impaired reparative fibrosis, leading to the development of cardiac rupture, and suggests a protective role of DCs during the post-MI cardiac repair process.<sup>29</sup> In humans, women amplify D-series resolvins biosynthesis compared with men to terminate systemic inflammation induced by typhoid vaccine, which confirms sex-specific SPM differences.<sup>4</sup> In mice, male and female equally biosynthesized SPMs with leukocyte expressed lipoxygenase activation after MI. However, although the female mice have increased inflammatory cytokines (*TNF-α*, *IL-1β*, *ARG-1*, and *MRC-1*) within the infarcted heart at day 1 after MI, the males have increases of the same cytokines within the spleen, indicating a difference in cardinal reaction of inflammation or reaction time between the male and female mice. This could also explain the lower rupture rates in female mice. Female mice also have a higher expression of receptors (*ALX/FPR2* and *EP4*) within the LVI at MI-d1, indicating an increased ability to bind to both pro-inflammatory and proresolving ligands, supporting the

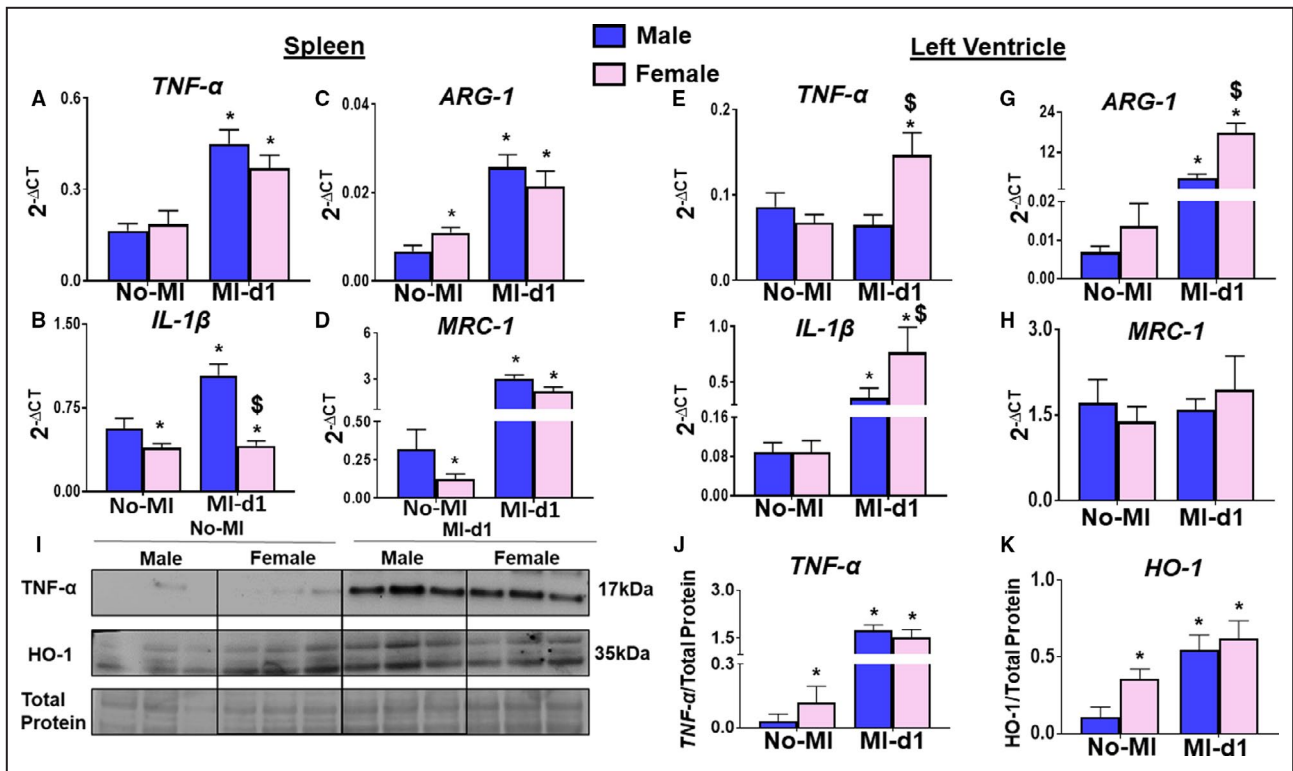


**Figure 8. Male mice have increased expression of cytokines in the spleen, female mice have increased expression of cytokines in the left ventricle.**

(A-D) Bar graphs of increased tumor necrosis factor (*TNF-α*), interleukin (*IL-1β*), Arginase 1 (*ARG-1*), Mannose Receptor C-Type 1 (*MRC-1*) in the spleen of male mice from no-MI to MI-d1. (E-H) Bar graphs of increased *TNF-α*, *IL-1β*, *ARG-1*, *MRC-1* in the left ventricle of female mice from no-MI to MI-d1. no-MI: males (n=4), females (n=4); MI-d1: males (n=6), females (n=6); \**P*<0.05 compared with no-MI naïve controls, #*P*<0.05 vs male at respective time point. (I-K) Western representative and bar graphs of expression of *TNF-α* and heme oxygenase-1 (*HO-1*). [(n=3/group); \**P*<0.05 compared with no-MI naïve controls, \$*P*<0.05 vs male at respective time point.

cardiac repair and recovery of the myocardium. Pain and inflammation are an obvious response to injury and wound healing, particularly resolvin D5 as one of the SPM moiety control chemotherapy-induced pain in females compared with males; thus, additional SPM investigation is warranted for precise and personnel sex-specific treatment.<sup>38</sup>

Cardiac healing after a heart attack is marked with overlapping inflammation and resolution processes that are initiated when leukocytes arrive at the site of infarction.<sup>12</sup> Historically, the resolution was considered as a passive event not considered as an active program and is coordinated by immune responsive leukocyte expressed lipoxygenase activation and interaction with essential fatty acids.<sup>12,39,40</sup> Quantitative analyses of leukocyte-directed SPMs (D-E series resolvins, protectins, maresins, and lipoxins) and cytochrome P450 epoxygenases mediated EETs suggest that male and female mice equally respond to the biosynthesis of SPMs. Of note, females biosynthesize higher levels of 11, 12 EETs compared with males. EETs manage microenvironment during inflammatory response, which favors macrophage reparative phenotype essential for

cardiac healing and repair.<sup>22,41,42</sup> The improved cardiac function and better survival in young risk-free female mice is attributable to the confounding factors associated with endogenous biosynthesis of the EET-enriched microenvironment. In this report, females mice have a longer survival with HF with a similar prevalence of HF than males. However, the outcome may change when various other risk factors (ie, processed and packed food intake, age, comedication, and metabolic defects) exist in preclinical or clinical setting.<sup>21,23,43,44</sup> Several reports have only studied mice at a young age, and it remains unknown if sex differences occur in other studies when research extends to aging animals with overlapping risk factors, such as obesity, insulin resistance, hyperglycemia, or high blood pressure.<sup>2</sup>

### Strengths

The presented study provided sex-specific temporal evidence with quantitative levels of bioactive lipid mediators in AHF and CHF. Survival, functional recovery, and leukocyte-directed cardiac repair that showed sex-specific signs of fine-tuned physiological inflammation

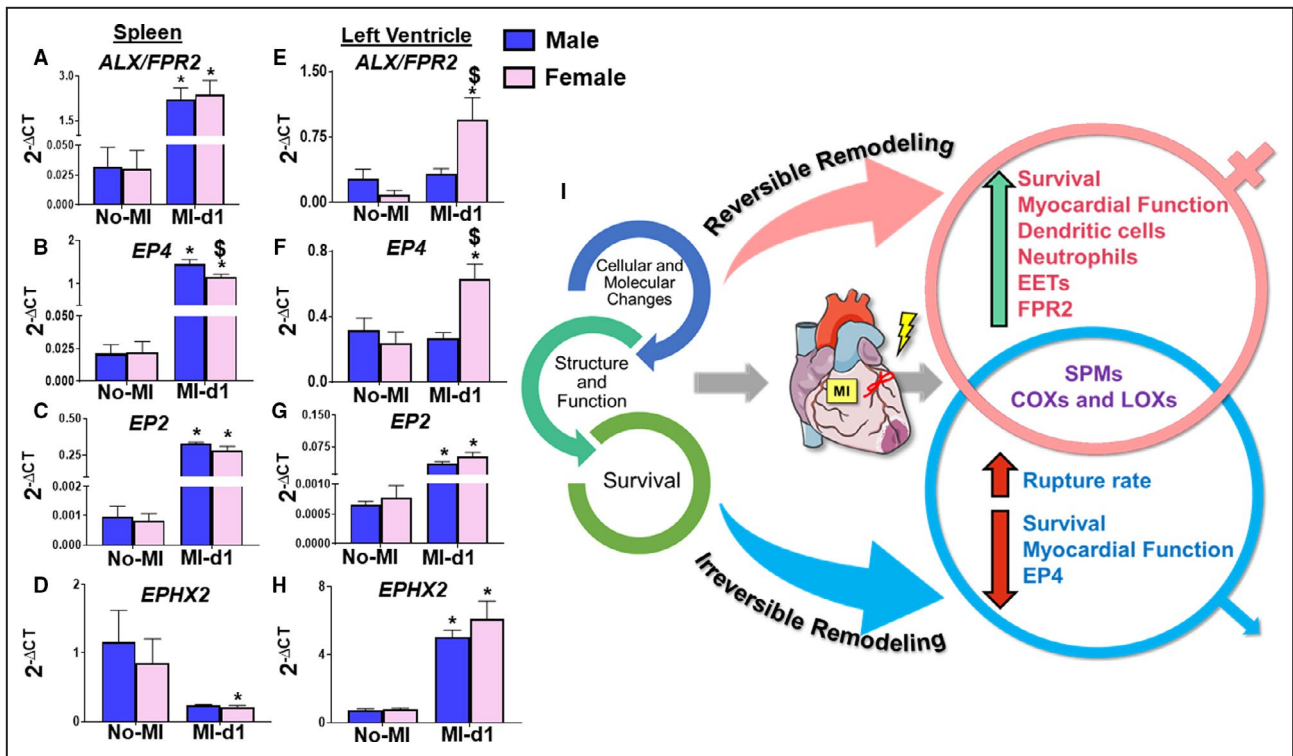


**Figure 9. Both sexes have differential expressions of receptors and enzymes in the spleen and left ventricle.** (A–D) Bar graphs of differential levels of *N*-formyl peptide receptor 2 (ALX/FPR2), prostaglandin E2 receptor 4 (EP4), Prostaglandin E2 receptor 2 (EP2), Epoxide Hydrolase 2 (EPHX2) in the spleen of male and female mice from no-MI to MI-d1. (E–H) Bar graphs of increased levels of ALX/FPR2, EP4, EP2, EPHX2 in the left ventricle of female mice from no-MI to MI-d1. no-MI: males (n=4), females (n=4); MI-d1: males (n=6), females (n=6); \*P<0.05 vs no-MI naïve controls, §P<0.05 vs male at respective time point. (I) Summary sketch showing the overall survival, function, and structure, and cellular and molecular changes between male and female mice in cardiac repair process.

in female mice without the risk factors that are common in a clinical setting (Figure 9I).

### Limitations and Perspective

In women, estrogen levels and leukocyte activity during the menstrual, proliferative, and secretory phases of menstrual cycle vary and remain uncovered in mice cardiac injury experiments.<sup>45</sup> In addition, the significance of some sex-related phenotype diversities warrants further investigation.

### Sources of Funding

The research reported in this publication was supported by the National Institutes of Health (HL132989 and HL144788 to Dr Halade). We acknowledge support from Mouse Cardiovascular Core Vevo 3100 Mouse Ultrasound Facility for this project. Dr Serhan is supported by Program Project 5 P01 GM095467 from the National Institutes of Health/National Institute of General Medical Sciences.

### Disclosures

None.

### Supplementary Materials

Figures S1–S6

### ARTICLE INFORMATION

Received December 31, 2019; accepted March 11, 2020.

#### Affiliations

From the Division of Cardiovascular Sciences, Department of Medicine, University of South Florida, Tampa, FL (A.B.P., V.K., G.V.H.); and Center for Experimental Therapeutics and Reperfusion Injury, Department of Anesthesiology, Perioperative and Pain Medicine, Brigham and Women's Hospital, Harvard Medical School, Boston, MA (C.N.S.).

#### Acknowledgments

Authors acknowledge the Servier Medical Art Gallery (creative common license) that was used to illustrate study design and summary figures in the article.

### REFERENCES

- Blenck CL, Harvey PA, Reckelhoff JF, Leinwand LA. The importance of biological sex and estrogen in rodent models of cardiovascular health and disease. *Circ Res*. 2016;118:1294–1312.
- Halade GV, Kain V. Obesity and cardiometabolic defects in heart failure pathology. *Compr Physiol*. 2017;7:1463–1477.
- Canto JG, Rogers WJ, Goldberg RJ, Peterson ED, Wenger NK, Vaccarino V, Kiefe CI, Frederick PD, Sopko G, Zheng Z-J, Investigators N. Association of age and sex with myocardial infarction symptom presentation and in-hospital mortality. *JAMA*. 2012;307:813–822.
- Rathod KS, Kapil V, Velmurugan S, Khambata RS, Siddique U, Khan S, Van Eijl S, Gee LC, Bansal J, Pitrola K, et al. Accelerated resolution of inflammation underlies sex differences in inflammatory responses in humans. *J Clin Invest*. 2017;127:169–182.

5. Lerner DJ, Kannel WB. Patterns of coronary heart disease morbidity and mortality in the sexes: a 26-year follow-up of the Framingham population. *Am Heart J*. 1986;111:383–390.
6. Bruder-Nascimento T, Ekeledo OJ, Anderson R, Le HB, Belin de Chantemèle EJ. Long term high fat diet treatment: an appropriate approach to study the sex-specificity of the autonomic and cardiovascular responses to obesity in mice. *Front Physiol*. 2017;8:32.
7. Murphy E. Estrogen signaling and cardiovascular disease. *Circ Res*. 2011;109:687–696.
8. Regitz-Zagrosek V, Kararigas G. Mechanistic pathways of sex differences in cardiovascular disease. *Physiol Rev*. 2017;97:1–37.
9. Pullen AB, Jadapalli JK, Rhourri-Frih B, Halade GV. Re-evaluating the causes and consequences of non-resolving inflammation in chronic cardiovascular disease. *Heart Fail Rev*. 2020;25:381–391.
10. DeLeon-Pennell KY, Lindsey ML. Somewhere over the sex differences rainbow of myocardial infarction remodeling: hormones, chromosomes, inflammasome, oh my. *Expert Rev Proteomics*. 2019;16:933–940.
11. DeLeon-Pennell KY, Ero OK, Ma Y, Padmanabhan Iyer R, Flynn ER, Espinoza I, Musani SK, Vasan RS, Hall ME, Fox ER, Lindsey ML. Glycoproteomic profiling provides candidate myocardial infarction predictors of later progression to heart failure. *ACS Omega*. 2019;4:1272–1280.
12. Halade GV, Norris PC, Kain V, Serhan CN, Ingle KA. Splenic leukocytes define the resolution of inflammation in heart failure. *Sci Signal*. 2018;11:eaao1818.
13. Serhan CN, Levy BD. Resolvins in inflammation: emergence of the pro-resolving superfamily of mediators. *J Clin Invest*. 2018;128:2657–2669.
14. Fredman G, Spite M. Specialized pro-resolving mediators in cardiovascular diseases. *Mol Aspects Med*. 2017;58:65–71.
15. Tourki B, Halade G. Leukocyte diversity in resolving and nonresolving mechanisms of cardiac remodeling. *FASEB J*. 2017;31:4226–4239.
16. Halade GV, Tourki B. Specialized pro-resolving mediators directs cardiac healing and repair with activation of inflammation and resolution program in heart failure. *Adv Exp Med Biol*. 2019;1161:45–64.
17. Duffney PF, Falsetta ML, Rackow AR, Thatcher TH, Phipps RP, Sime PJ. Key roles for lipid mediators in the adaptive immune response. *J Clin Invest*. 2018;128:2724–2731.
18. Basil MC, Levy BD. Specialized pro-resolving mediators: endogenous regulators of infection and inflammation. *Nat Rev Immunol*. 2016;16:51–67.
19. Conte MS, Desai TA, Wu B, Schaller M, Werlin E. Pro-resolving lipid mediators in vascular disease. *J Clin Invest*. 2018;128:3727–3735.
20. Halade GV, Kain V, Ingle KA. Heart functional and structural compendium of cardioplemic and cardiorenal networks in acute and chronic heart failure pathology. *Am J Physiol Heart Circ Physiol*. 2018;314:H255–H267.
21. Lopez EF, Kabarowski JH, Ingle KA, Kain V, Barnes S, Crossman DK, Lindsey ML, Halade GV. Obesity superimposed on aging magnifies inflammation and delays the resolving response after myocardial infarction. *Am J Physiol Heart Circ Physiol*. 2015;308:H269–H280.
22. Halade GV, Kain V, Tourki B, Jadapalli JK. Lipoxygenase drives lipidomic and metabolic reprogramming in ischemic heart failure. *Metabolism*. 2019;96:22–32.
23. Halade GV, Kain V, Black LM, Prabhu SD, Ingle KA. Aging dysregulates D- and E-series resolvins to modulate cardioplemic and cardiorenal network following myocardial infarction. *Aging (Albany NY)*. 2016;8:2611–2634.
24. Halade GV, Kain V, Serhan CN. Immune responsive resolvin D1 programs myocardial infarction-induced cardiorenal syndrome in heart failure. *FASEB J*. 2018;32:3717–3729.
25. Halade GV, Kain V, Wright GM, Jadapalli JK. Subacute treatment of carprofen facilitate splenocardiac resolution deficit in cardiac injury. *J Leukoc Biol*. 2018;104:1173–1186.
26. Kain V, Ingle KA, Colas RA, Dalli J, Prabhu SD, Serhan CN, Joshi M, Halade GV. Resolvin D1 activates the inflammation resolving response at splenic and ventricular site following myocardial infarction leading to improved ventricular function. *J Mol Cell Cardiol*. 2015;84:24–35.
27. Dalli J, Serhan CN. Specific lipid mediator signatures of human phagocytes: microparticles stimulate macrophage efferocytosis and pro-resolving mediators. *Blood*. 2012;120:e60–e72.
28. Colas RA, Shinohara M, Dalli J, Chiang N, Serhan CN. Identification and signature profiles for pro-resolving and inflammatory lipid mediators in human tissue. *Am J Physiol Cell Physiol*. 2014;307:C39–C54.
29. Nagai T, Honda S, Sugano Y, Matsuyama T-a, Ohta-Ogo K, Asaumi Y, Ikeda Y, Kusano K, Ishihara M, Yasuda S, et al. Decreased myocardial dendritic cells is associated with impaired reparative fibrosis and development of cardiac rupture after myocardial infarction in humans. *J Am Heart Assoc*. 2014;3:e000839. DOI: 10.1161/JAHA.114.000839.
30. Cowie MR, Zakeri R. Preventing heart failure at the population level: conventional cardiovascular risk factor management should continue. *JACC Heart Fail*. 2019;7:214–216.
31. Magnussen C, Niiranen TJ, Ojeda FM, Gianfagna F, Blankenberg S, Vartiainen E, Sans S, Pasterkamp G, Hughes M, Costanzo S, et al. Sex-specific epidemiology of heart failure risk and mortality in Europe: results from the biomarcare consortium. *JACC Heart Fail*. 2019;7:204–213.
32. Barrett-Connor E. Sex differences in coronary heart disease: why are women so superior? The 1995 ancel keys lecture. *Circulation*. 1997;95:252–264.
33. Ziaeiyan B, Kominski Gerald F, Ong Michael K, Mays Vickie M, Brook Robert H, Fonarow Gregg C. National differences in trends for heart failure hospitalizations by sex and race/ethnicity. *Circ Cardiovasc Qual Outcomes*. 2017;10:e003552.
34. DeLeon-Pennell KY, Mouton AJ, Ero OK, Ma Y, Padmanabhan Iyer R, Flynn ER, Espinoza I, Musani SK, Vasan RS, Hall ME, et al. LXR/RXR signaling and neutrophil phenotype following myocardial infarction classify sex differences in remodeling. *Basic Res Cardiol*. 2018;113:40.
35. Cherpokova D, Jouve CC, Liberos S, DeRoo EP, Chu L, de la Rosa X, Norris PC, Wagner DD, Serhan CN. Resolvin D4 attenuates the severity of pathological thrombosis in mice. *Blood*. 2019;134:1458–1468.
36. Sager HB, Kessler T, Schunkert H. Monocytes and macrophages in cardiac injury and repair. *J Thorac Dis*. 2017;9:S30–S35.
37. Gallego-Colon E, Sampson RD, Sattler S, Schneider MD, Rosenthal N, Tonkin J. Cardiac-restricted IGF-1Ea overexpression reduces the early accumulation of inflammatory myeloid cells and mediates expression of extracellular matrix remodeling genes after myocardial infarction. *Mediators Inflamm*. 2015;2015:484357.
38. Luo X, Gu Y, Tao X, Serhan CN, Ji RR. Resolvin D5 inhibits neuropathic and inflammatory pain in male but not female mice: distinct actions of D-series resolvins in chemotherapy-induced peripheral neuropathy. *Front Pharmacol*. 2019;10:745.
39. Serhan CN. Pro-resolving lipid mediators are leads for resolution physiology. *Nature*. 2014;510:92–101.
40. Seubert JM, Sinal CJ, Graves J, DeGraff LM, Bradbury JA, Lee CR, Goralski K, Carey MA, Luria A, Newman JW, et al. Role of soluble epoxide hydrolase in posts ischemic recovery of heart contractile function. *Circ Res*. 2006;99:442–450.
41. Kain V, Ingle KA, Kabarowski J, Barnes S, Limdi NA, Prabhu SD, Halade GV. Genetic deletion of 12/15 lipoxygenase promotes effective resolution of inflammation following myocardial infarction. *J Mol Cell Cardiol*. 2018;118:70–80.
42. Nayeem MA. Role of oxylipins in cardiovascular diseases. *Acta Pharmacol Sin*. 2018;39:1142–1154.
43. Kain V, Van Der Pol W, Mariappan N, Ahmad A, Eipers P, Gibson DL, Gladine C, Vigor C, Durand T, Morrow C, Halade GV. Obesogenic diet in aging mice disrupts gut microbe composition and alters neutrophil: lymphocyte ratio, leading to inflamed milieu in acute heart failure. *FASEB J*. 2019;33:6456–6469.
44. Kain V, Ingle KA, Kachman M, Baum H, Shanmugam G, Rajasekaran NS, Young ME, Halade GV. Excess omega-6 fatty acids influx in aging drives metabolic dysregulation, electrocardiographic alterations, and low-grade chronic inflammation. *Am J Physiol Heart Circ Physiol*. 2018;314:H160–H169.
45. Bain BJ, England JM. Variations in leucocyte count during menstrual cycle. *Br Med J*. 1975;2:473–475.

# **Supplemental Material**



**Figure S1. (A)** Gating strategy for flow cytometry. **(B-C)** Donuts pie chart showing the survival rates of both sexes in acute and chronic HF.

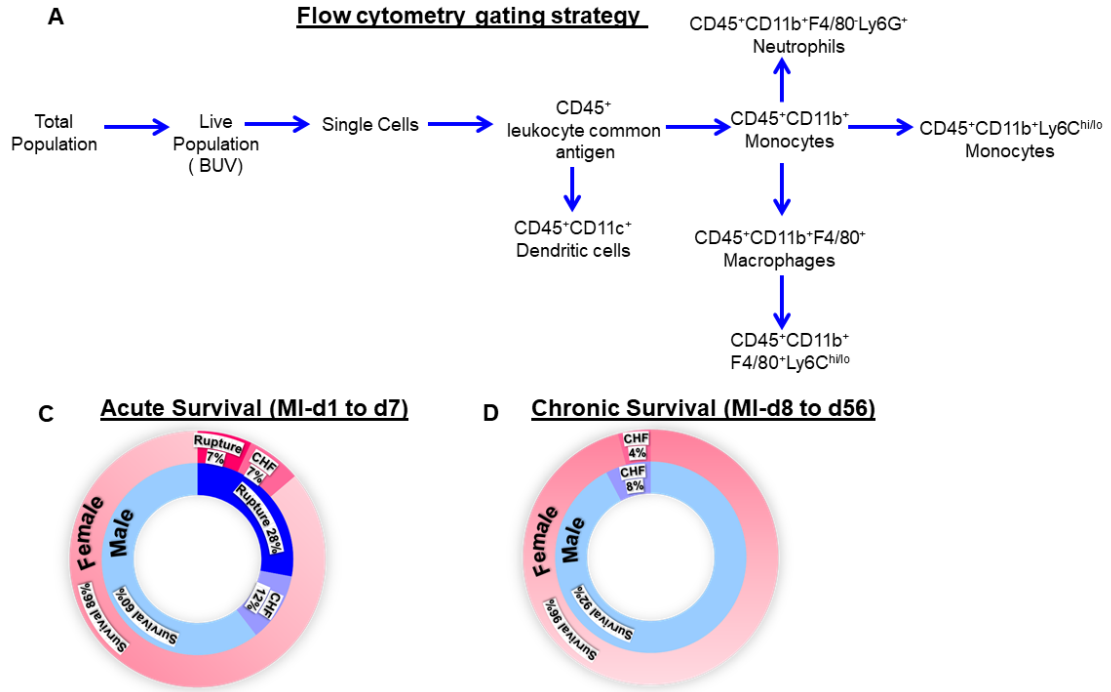


**Figure S2. Heat map showing differential quantity of specialized pro-resolving mediators (SPMs) and epoxyeicosatrienoic acid (EETs) in male and female mice.**

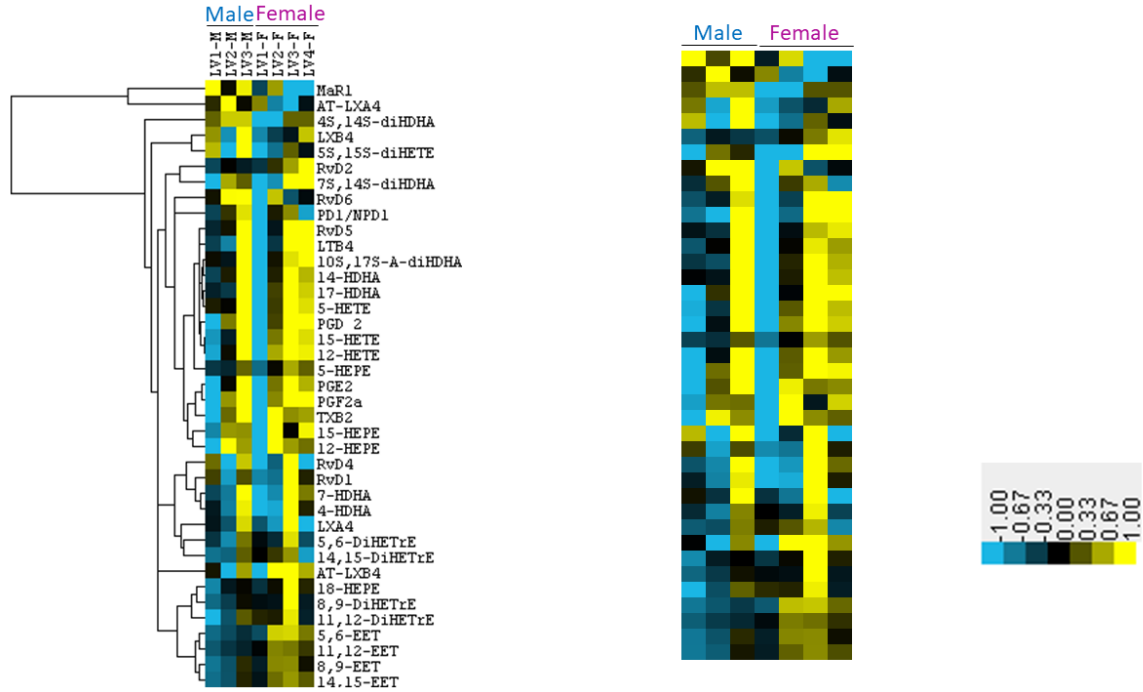


**Figure S3. Biosynthesis of arachidonic acid (AA)-derived proinflammatory mediators in male and female mice post-MI. (A) Pie chart showing the AA-derived proinflammatory mediators in the left ventricle of male mice at MI-d1. (B) Pie chart showing the AA-derived proinflammatory mediators in the left ventricle of female mice at MI-d1. (C) Bar graph showing AA-derived proinflammatory mediators of the left ventricle at MI-d1 of male and female mice. MI-d1: males (n=3), females (n=4).**

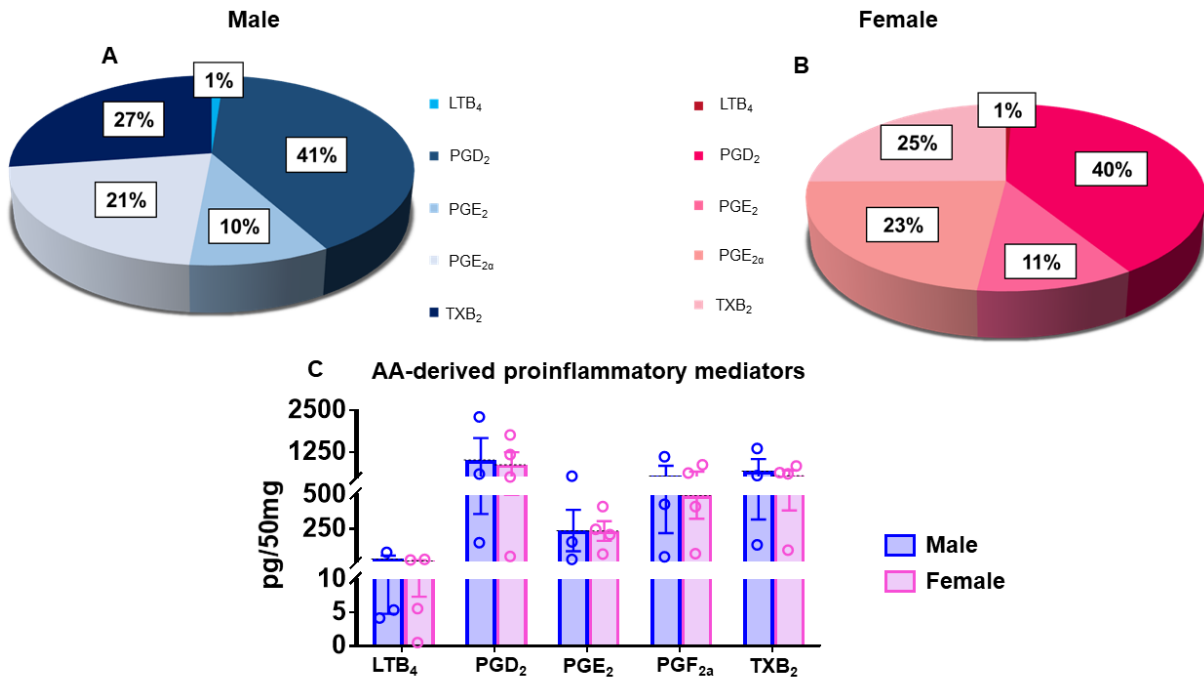


**Figure S4. Endogenous biosynthesis of docosahexaenoic acid (DHA) and eicosapentaenoic acid (EPA)-derived SPM precursors in male and female mice post-MI (A)** Pie chart showing the DHA and EPA precursors in the left ventricle of male mice at MI-d1. **(B)** Pie chart showing the DHA and EPA precursors in the left ventricle of female mice at MI-d1. **(C)** Bar graph showing DHA and EPA precursors of the left ventricle at MI-d1 of male and female mice. MI-d1: males (n=3), females (n=4).

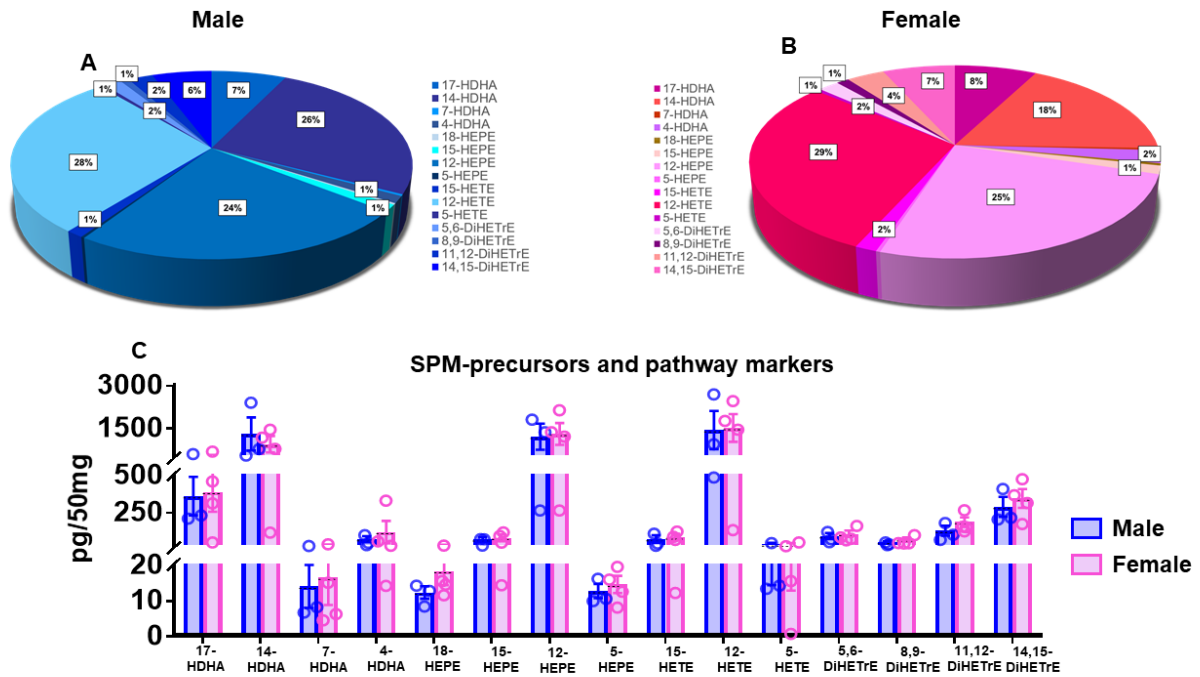


**Figure S5. Structural changes in cardiomyocyte area.** Wheat germ agglutinin (WGA) staining showing cardiomyocyte area in male and female mice. WGA = green, Hoechst = blue, [No-MI: males (n=4), females (n=4); MI-d1: males (n=5), females (n=6); MI-d56: males (n=4), females (n=4)].

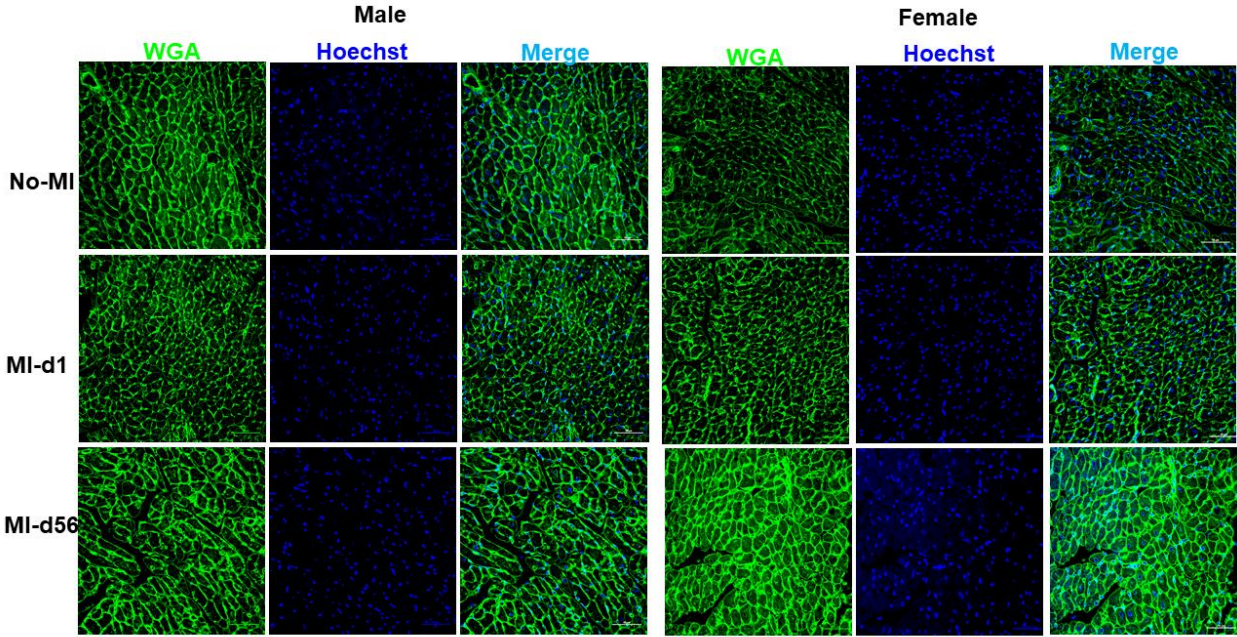


**Figure S6. Female mice have higher reparative macrophages (MΦ) compared to male mice post-MI. (A)** Plot showing macrophages at No-MI, MI-d1, MI-d3, MI-d5, and MI-d56 in male and female mice. **(B)** Plot showing Ly6C<sup>lo</sup> and Ly6C<sup>hi</sup> macrophages at No-MI, MI-d1, MI-d3, MI-d5, and MI-d56 in male and female mice. **(C-E)** Line graphs showing the percentage of the cell population for CD11b, Ly6C<sup>hi</sup>MΦ, and Ly6C<sup>lo</sup>MΦ. [No-MI: males (n=4), females (n=4); MI-d1: males (n=5), females (n=6); \$p<0.05 vs male at respective time point; \*p<0.05 compared to no-MI naïve controls.

